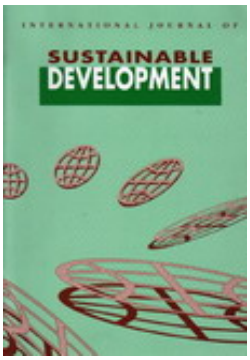

International Journal of Sustainable Development

ISSN online: 1741-5268 - ISSN print: 0960-1406
https://www.inderscience.com/ijsd

Intelligent monitoring method for agricultural nonpoint source pollution based on remote sensing image changes

Tiebo Sun, Meng Li, Weibing Wang, Chunyue Liu

DOI: 10.1504/IJSD.2024.10062822

Article History:

Received:	11 September 2023
Last revised:	05 January 2024
Accepted:	09 January 2024
Published online:	15 July 2024

Intelligent monitoring method for agricultural nonpoint source pollution based on remote sensing image changes

Tiebo Sun*, Meng Li and Weibing Wang

School of Intelligent Manufacturing,
Jiangsu Food & Pharmaceutical Science College,
Huai'an City, Jiangsu Province, 223003, China
Email: sieo2023@163.com
Email: 21494571@qq.com
Email: 1165508648@qq.com
*Corresponding author

Chunyue Liu

College of Automotive Engineering,
Jiangsu Vocational College of Electronics and Information,
Huai'an City, Jiangsu Province, 223003, China
Email: 519441240@qq.com

Abstract: To address issues related to insufficient monitoring coverage, inaccurate measurement of pollution concentration, and inadequate load monitoring using traditional methods, an intelligent monitoring method for agricultural non-point source pollution based on remote sensing image changes is proposed. Utilising Landsat ETM+ remote sensing imagery, a multi-layer perceptron algorithm is employed to detect and identify agricultural non-point source pollution areas. The Min-Cut algorithm is used for remote sensing image segmentation of agricultural non-point source pollution targets. Remote sensing image changes are detected based on the segmentation results and difference diagram. Intelligent monitoring of agricultural non-point source pollution is achieved by combining the detection results of remote sensing image changes with relevant monitoring indicators. Experimental findings demonstrate that the proposed method achieves a monitoring coverage rate exceeding 96.3%, the mean accuracy of pollution concentration monitoring is 97.1%, the maximum accuracy of pollution load monitoring is 99.3%.

Keywords: remote sensing image changes; agricultural non-point source pollution; intelligent monitoring; Landsat ETM+ remote sensing images; min-cut algorithm; difference diagram; monitoring indicators.

Reference to this paper should be made as follows: Sun, T., Li, M., Wang, W. and Liu, C. (2024) 'Intelligent monitoring method for agricultural nonpoint source pollution based on remote sensing image changes', *Int. J. Sustainable Development*, Vol. 27, No. 3, pp.280–297.

Biographical notes: Tiebo Sun received his PhD in School of Technology from Beijing Forestry University in 2021. He is currently an Associate Professor in the School of Intelligent Manufacturing of Jiangsu Food &

Pharmaceutical Science College. His research interests include laser measuring technology, machine vision inspection systems, and image processing.

Meng Li received his Master's degree in School of Electrical Engineering from Jiangsu University in 2012. He is currently an Associate Professor in the School of Intelligent Manufacturing of Jiangsu Food & Pharmaceutical Science College. His research interests include electrical automation, machine vision inspection systems, and mechanical engineering.

Weibing Wang received his Bachelor's degree in College of electrical engineering from Southeast University in 1995. He is currently a Professor in the School of Intelligent Manufacturing of Jiangsu Food & Pharmaceutical Science College. His research interests include electronic technique and mechanical engineering.

Chunyue Liu received her Master's degree in School of Public Relations from Southwest Jiaotong University in 2009. She is currently an Associate Professor in the College of Automotive Engineering of Jiangsu Vocational College of Electronics and Information. Her research interests include laser measuring technology and machine vision inspection systems.

1 Introduction

Agricultural non-point source pollution refers to pollution caused by various agricultural activities, including farming practices, livestock farming, and rural activities. The pollutants enter water bodies through channels such as rainwater and surface runoff, causing negative impacts on the water environment (Niu et al., 2022). Improper management, unsustainable resource utilisation, and inadequate environmental awareness in agricultural activities contribute to the occurrence (Li et al., 2022). Implementing scientifically sound and sustainable cultivation practices is essential for mitigating agricultural non-point source pollution, pesticide and fertiliser use management, livestock waste treatment, and irrigation water resource management (Wan, 2021; Lin and Pan, 2020). Real-time monitoring pollution yields valuable information for farmers and agricultural producers, enabling them to enhance their management practices, minimise pollutant emissions, and reduce waste in agricultural activities. By promptly assessing the distribution and appropriate control measures can be implemented to steer agricultural development, manage water resources, and elevate the standards of sustainable agricultural practices.

Zhang et al. (2022) proposed an intelligent monitoring method based on the RAISR algorithm. Through the utilisation of drone aerial remote sensing system, we have the capacity to procure remote sensing images pertaining to water conservancy. In order to achieve accurate reconstruction of agricultural non-point source pollution images, advanced RAISR algorithms are used for preprocessing. In the learning stage, image generation filters are trained to optimise the reconstruction effect of the image. Furthermore, the technique of histogram analysis is employed to analyse remote sensing images, and the maximum cumulative variance method is used to determine the

appropriate threshold and calculate the basic parameters of remote sensing images. In order to achieve accurate segmentation of remote sensing images, the EM algorithm is used for multiple iterations to obtain the optimal parameters. By introducing a Gaussian mixture model and calculating t-link weights, the segmentation of remote sensing images was successfully achieved. Extract remote sensing features. Using this feature can more accurately monitor and grasp the situation, and output relevant monitoring results. However, in reality, this method has proven to be unreliable and inaccurate in effectively monitoring the concentration of pollutants stemming from agricultural non-point sources. Wang and Li (2022) proposed an intelligent monitoring method based on graph convolutional neural networks. Utilise multi-sensor collection of agricultural data to extract multivariate temporal data related to water quality from the collected data. Construct a graph structure using graph convolutional neural networks, connect farmland as nodes, and establish relationships between nodes. By training this graph, the network can automatically learn the characteristics and pollution propagation laws between nodes, and use the network to output relevant intelligent monitoring results. However, in real-world scenarios, it has been noted that the effectiveness of intelligent monitoring for agricultural non-point source pollution using this method falls short of expectations, with a significant gap between the achieved coverage rate and the anticipated goals. Xiang et al. (2022) proposed an intelligent monitoring method based on the Internet of Things cloud platform. Using multiple types of sensors to collect temperature, pH, and other types of data, and uploading them to the IoT monitoring center for centralised storage and processing. On the cloud platform, advanced data analysis and machine learning algorithms are used to process and analyse the collected data. By constructing models and training algorithms, the system can automatically identify the characteristics and patterns, thereby achieving intelligent monitoring. However, during implementation, significant issues have arisen with the accuracy of this method in monitoring the load of agricultural non-point source pollutants, rendering its practical application considerably ineffective.

A new intelligent monitoring method for agricultural non-point source pollution based on remote sensing image changes is proposed with the research goal of solving various problems existing in traditional methods. The coverage rate, accuracy rate of pollutant concentration monitoring, and accuracy rate of pollutant load monitoring are utilised as indicators to assess the effectiveness of this method. These indicators serve as conclusive measures to verify the method's efficacy. The intelligent monitoring method has the following innovative technological routes:

1 *Data source selection*: Using Landsat ETM+ remote sensing images as the data source, utilising its high-resolution and multispectral information, provides a reliable data foundation.

2 *Agricultural non-point source pollution target recognition*: Using multilayer perceptron (MLP) as a classification model, automatic recognition of agricultural non-point source pollution targets in remote sensing images is carried out.

3 *Remote sensing image segmentation processing*: Based on target recognition results, the Min Cut algorithm is used to segment remote sensing images, achieving effective extraction of targets and clear definition of boundaries.

4 *Remote sensing image change detection*: By utilising segmentation results and difference maps, one can ascertain the variations in agricultural non-point source pollution targets within remote sensing images. This information can then be leveraged to monitor and analyse the spatiotemporal distribution of pollutants.

5 *Intelligent monitoring and indicator analysis*: By combining agricultural non-point source pollution monitoring indicators, the remote sensing image change detection results and indicators are comprehensively analysed to achieve intelligent monitoring and comprehensive evaluation.

The experimental results indicate that the intelligent monitoring method by this innovative technology route has high coverage and accuracy. By employing this method, it is possible to accomplish comprehensive monitoring and management of non-point source pollution in farmland, providing important technical support and decision-making reference for environmental protection, sustainable development of farmland, and improvement of agricultural production efficiency.

2 Intelligent monitoring method for agricultural non-point source pollution

2.1 Pollution target recognition based on remote sensing images

The acquisition of remote sensing image data often presents various technical challenges and difficulties. One of the initial challenges is selecting suitable sensors that fulfil the specific research needs, while also grappling with the availability and accessibility of necessary data. Processing raw image data may require preprocessing and correction, including atmospheric correction, geometric correction, and radiation correction. In addition, there are various noise sources in remote sensing images, such as clouds, shadows, and atmospheric interference, which require denoising and restoration techniques for processing. Furthermore, to acquire a more comprehensive and precise understanding of the subject matter, it is imperative to ensure that all significant aspects are thoroughly examined, it is often necessary to fuse data from different sensors or multiple time points, which needs to address the differences in data format and consistency. Finally, remote sensing image data typically has a large number of spatial and temporal dimensions, requiring high-speed computing and storage systems to process and store large-scale data, as well as effective data management and querying. Landsat satellite, equipped with multispectral sensors, can obtain high-resolution image data in the visible and infrared bands (Zhao et al., 2022; Fan et al., 2022), providing rich surface information. The spatial resolution of Landsat images is usually between 15 m and 30 m, which means it can capture details of the surface and provide high accuracy (Ridwana et al., 2021; Li et al., 2011). In addition, Landsat data also provides long-term observation data for historical change analysis and monitoring.

Table 1 provides a comprehensive overview of the information obtained from the Landsat ETM+ remote sensing images.

Table 1 Landsat ETM+remote sensing image information

Name	*Resolution ratio/m*	*Wavelength/μm*	*Band*
Band 1	30	0.45~0.52	Blue-green band
Band 2	30	0.52~0.60	Green band
Band 3	30	0.63~0.69	Red band
Band 4	30	0.76~0.90	Near infrared band
Band 5	30	1.55~1.75	Mid infrared band
Band 6	60	10.40~12.50	Thermal infrared band
Band 7	30	2.08~2.35	Mid infrared band
PAN	15	0.52~0.90	Panchromatic band

Multilayer perceptron is an artificial neural network model commonly used to solve classification and regression problems. It consists of multiple neural layers, each of which processes inputs through weights and activation functions and passes them on to the next layer. By continuously adjusting weights and biases, MLP can learn complex nonlinear relationships between data (Shirazi and Toosi, 2023; Wu et al., 2022). In agricultural non-point source pollution target recognition, multi-layer perceptrons can be applied to image classification and target recognition tasks. By extracting features from Landsat ETM+remote sensing images as input, multi-layer perceptrons can learn feature representations of different categories and recognise targets such as farmland, crops, and water bodies. Figure 1 illustrates the structure of the multi-layer perceptron.

Figure 1 Multilayer perceptron structure

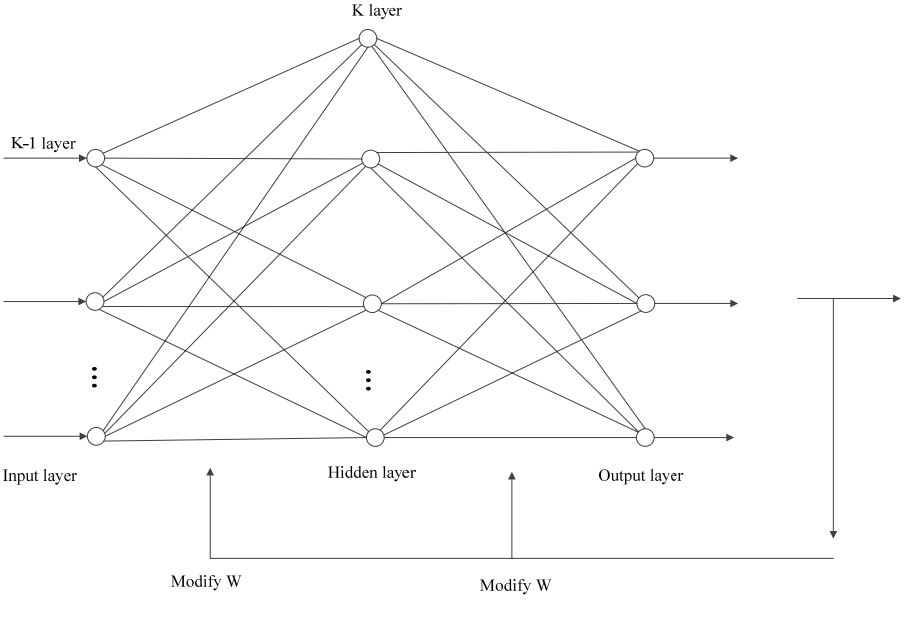

The mathematical model of a multi-layer perceptron is represented by the following formula:

$$Y = f\left[\sum_{i=1}^{n} W_i X_i - \theta\right] \tag{1}$$

In the above formula, X_i represents the *i*th Landsat ETM+remote sensing image, W_i is the weight of the *i*th neural network, and θ is the bias parameter.

The procedure for identifying agricultural non-point source pollution targets using multi-layer perceptrons is outlined below:

1 Set the initial value for weight W. For components with different weight coefficients $W = (W_1, W_2, \ldots, W_n)$, set a smaller zero random value of $W_1(0), W_2(0), \ldots, W_n(0)$. Then $W_i(t)$ represents the weight value on the *i*th input at t, $i = 1, 2, \ldots, n$.

2 Landsat ETM+remote sensing image $X = (X_1, X_2, \ldots, X_n)$, expected output is *d*.

3 Based on the constructed multi-layer perceptron mathematical model, the output is calculated, and the specific calculation results are as follows:

$$Y(t) = f\left[\sum_{i=1}^{n+1} W_i(t) X_i\right] \tag{2}$$

4 Calculate the error *e* based on the actual output, which is calculated using the following formula:

$$e = d - Y(t) \tag{3}$$

5 The weight value is modified based on the *e* values calculated by formula (3), and the specific results are as follows:

$$W_i(t+1) = W_i(t) + \eta \cdot e \cdot X_i \tag{4}$$

In formula, η is the rate of change in weight, and $0 < \eta \leq 1$. If the actual output is consistent with the expected value d, the following formula holds:

$$W_i(t+1) = W_i(t) \tag{5}$$

6 For the first Landsat ETM+remote sensing image X_2, if its actual output and expected output remain consistent, perform the steps (1)–(5) above for the second sample X_2 until all samples meet the requirements. The obtained remote sensing image can yield recognition results for agricultural non-point source pollution targets by employing the following formula:

$$Y = f\left[\sum_{i=1}^{n+1} W_i(t+1) X_i\right] \tag{6}$$

2.2 Remote sensing image segmentation

The process of segmenting agricultural non-point source pollution targets from remote sensing images holds paramount significance. It serves as a fundamental step in precisely pinpointing the targets, elevating the reliability and accuracy of target recognition, and

establishing a solid basis for subsequent analysis and decision-making, thereby playing a pivotal role in the overall process. It is one of the key steps for monitoring and managing. Henceforth, this paper synergistically merges the findings from pollution target recognition, elucidated in Section 2.1, with the process of segmenting Landsat ETM+ remote sensing images.

Assuming that Landsat ETM+remote sensing images are represented by $z=(z_1,\ldots,z_n,\ldots,z_N)$, and z_n represents the greyscale value of each pixel in the remote sensing image. Definition $\alpha=(\alpha_1,\ldots,\alpha_n,\ldots,\alpha_N)$, where $\alpha_n\in\{0,1\}$. Assign a value of k_n, $k_n\in\{1,\ldots,K\}$ to each pixel *n*, indicating which Gaussian model the pixels belong to. Therefore, for an entire Landsat ETM+remote sensing image, there is $k=(k_1,\ldots,k_n,\ldots,k_N)$.

Establish the minimum energy function for Landsat ETM+remote sensing images, which is represented by the following formula:

$$\hat{\alpha}=arg\min_{\alpha}E(\alpha,k,\theta,z) \tag{7}$$

In the above formula, θ represents the parameters of the Gaussian model and $E(\alpha,k,\theta,z)$ represents the Gibbs energy parameter, which is represented by the following formula:

$$E(\alpha,k,\theta,z)=U(\alpha,k,\theta,z)+V(\alpha,z) \tag{8}$$

Let $V(\alpha,z)$ represent the histogram illustrating the distribution of greyscale frequency. The probability of measuring the pixels belonging to the foreground and background is defined as follows:

$$\mathrm{U}(\alpha,k,\theta,z)=\sum_{n}D(\alpha_n,k_n,\theta,z_n) \tag{9}$$

$$D(\alpha_n,k_n,\theta,z_n)=-\log p(z_n|\alpha_n,k_n,\theta)-\log\pi(\alpha_n,k_n) \tag{10}$$

In the above formula, $\pi(\alpha_n,k_n)$ represents the weight of the Gaussian component, and $p(z_n|\alpha_n,k_n,\theta)$ represents the Gaussian distribution of the three-dimensional Gaussian model, namely:

$$p(z_n|\alpha_n,k_n,\theta)=\frac{1}{\sqrt{(2\pi)^d|\Sigma|}}\exp\left[-\frac{1}{2}(z_n-\mu)'\Sigma^{-1}(z_n-\mu)\right] \tag{11}$$

In the above formula, $d=3$, $\Sigma=\Sigma(\alpha_n,k_n)$, $\mu=\mu(\alpha_n,k_n)$ represents the Gaussian component, and z_n represents the RGB information of pixels in Landsat ETM+remote sensing images, which is a three-dimensional vector. By substituting it into formula (11), the following results can be obtained:

$$\begin{aligned}D(\alpha_n,k_n,\theta,z_n)=&-log\pi(\alpha_n,k_n)+\frac{1}{2}logdet\sum(\alpha_n,k_n)\\&+\frac{1}{2}\left[z_n-\mu(\alpha_n,k_n)\right]'\sum(\alpha_n,k_n)^{-1}\left[z_n-\mu(\alpha_n,k_n)\right]\end{aligned} \tag{12}$$

In the above formula, $V(\alpha, z)$ represents the difference parameter between pixel points and surrounding pixel points, and the specific calculation formula is as follows:

$$V(\alpha, z) = \gamma \sum_{(m,n)\in C} [\alpha_n \neq \alpha_m] \exp\left[-\beta \| z_m - z_n \|^2\right] \tag{13}$$

In formula (13), β is the pixel mean, and C is the set formed by combining a certain pixel point with its neighbouring pixels.

1 The Gaussian component in the Gaussian model is assigned to each pixel, and the results are as follows:

$$\hat{k}_n = arg \min_{k_n} D_n(\alpha_n, k_n, \theta, z_n) \tag{14}$$

2 Given the outcomes of the aforementioned analysis, the parameters of the Gaussian model were acquired and fine-tuned, leading to the subsequent results:

$$\hat{\theta} = arg \min_{\theta} U(\alpha, k, \theta, z) \tag{15}$$

3 By leveraging the Min-Cut algorithm, the remote sensing image segmentation of agricultural non-point source pollution targets yields the following results:

$$F = \arg\min_{\alpha} E\left(\alpha, \hat{k}_n, \hat{\theta}, z\right) \tag{16}$$

2.3 Remote sensing image change detection

The process of remote sensing image change detection involves using multi temporal remote sensing image data to identify and evaluate the changes of these targets. This is achieved by comparing images captured at different time points and analysing the variations observed between them. This method can determine whether the target has changed by analysing the differences in pixel values or other specific change indicators in the image. By detecting changes in remote sensing images, valuable insights can be gained into the evolving patterns of agricultural non-point source pollution targets. These changes can include the expansion of farmland, alterations in crops, shifts in water areas, and more. Such analysis aids in evaluating the environmental impact of agricultural activities and assessing the rationality of resource utilisation. Figure 2 illustrates the architecture of the change detection system for remote sensing images.

Assuming that two remote sensing images at different time points are represented by images 1 and 2 respectively, a multi difference operator, namely LR difference map and MR difference map, is used for decision fusion to generate a difference map. Unsupervised clustering functions are used for pre classification, and pixels are divided into modified, unchanged, and invariant classes, and further operations are carried out. Subsequently, the frequency domain analysis FDA module was used to convert it into a frequency domain operation, and the DCT function was used for frequency domain conversion. The DCT coefficients were inputted into the GLU for selection. The output results were then obtained through two fully connected layers to obtain the variation difference diagram at different time points using remote sensing images 1 and 2, respectively, in order to achieve remote sensing image change detection of agricultural non-point source pollution targets.

Figure 2 Architecture for detecting changes in remote sensing images of agricultural non-point source pollution targets (see online version for colours)

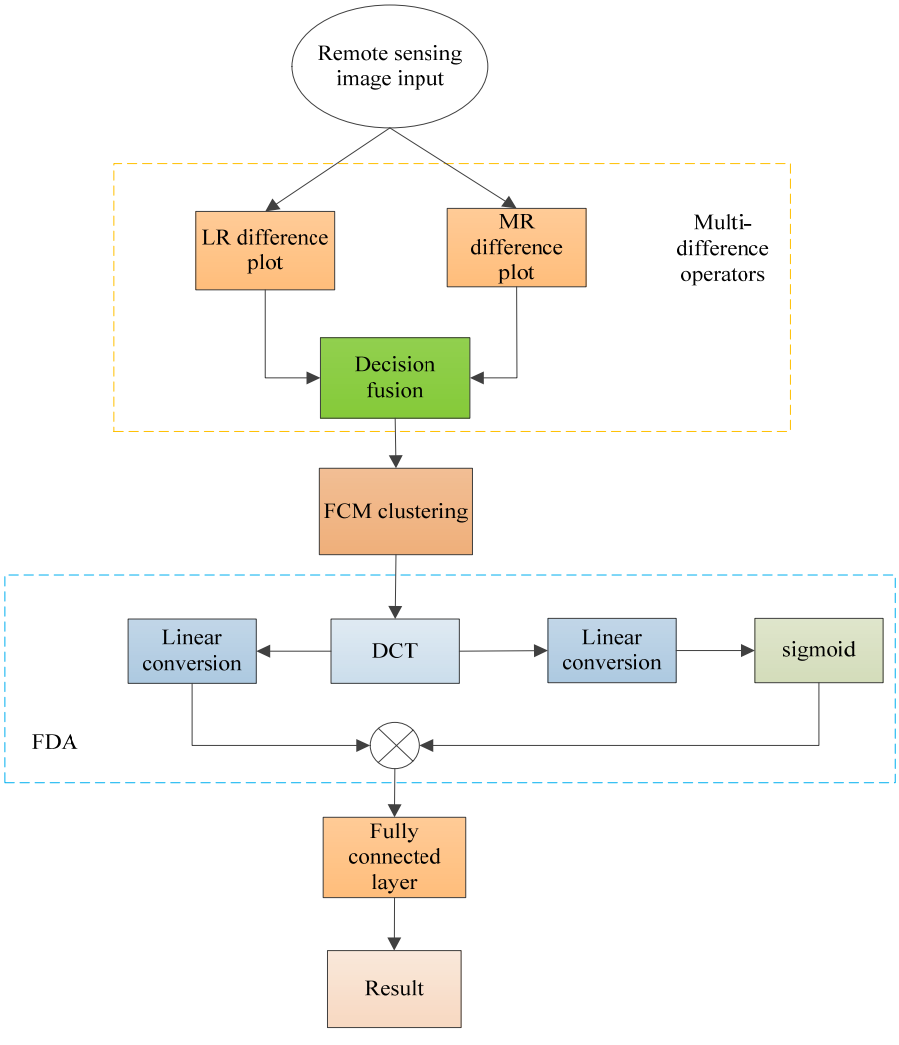

1 *Multi difference operator module*

The logarithmic ratio operator is an effective tool for converting the multiplicative random noise present in remote sensing images of agricultural non-point source pollution targets into additive noise. This transformation mitigates the impact of noise, allowing for more accurate and reliable image analysis and interpretation. The difference image generated by it is transformed and nonlinear shrinkage is achieved, which is better when the proportion of unchanged areas is large. The difference image generated by it is represented by the following formula:

$$D_{LR}(x) = \left| log \frac{I_2(x) + C}{I_1(x) + C} \right| \tag{17}$$

In formula (17), $I_1(x)$ and $I_2(x)$ represents the intensity values of images 1 and 2 at spatial position x, respectively, and C represents a non-zero constant.

The mean ratio operator can suppress individual outliers to a certain extent, but its effect is average for areas with a large amount of noise accumulation. The difference graph introducing the mean ratio operator is represented by the following formula:

$$D_{MR}(x) = 1 - \frac{min\left(\overline{I}_1(x), \overline{I}_2(x)\right)}{max\left(\overline{I}_1(x), \overline{I}_2(x)\right)} \tag{18}$$

In the above formula, $\overline{I}_1(x)$ and $\overline{I}_2(x)$ represent the intensity of images 1 and 2 after mean filtering.

Combining the advantages of the above operators and considering the individual and neighbourhood information in remote sensing images, this paper proposes a multi difference operator method that combines the logarithmic ratio operator and the mean ratio operator to generate a difference map. The generated difference map is represented by the following formula:

$$D_{MD}(x) = \alpha D_{LR}(x) + (1-\alpha) D_{MR}(x) \tag{19}$$

In the above formula, α represents the fusion parameters.

2 *FCM clustering module*

Fuzzy mean clustering (FMC) is an extended method based on fuzzy C-means clustering (FCM). FMC introduces the fuzzy mean function on the basis of FCM, optimises clustering results by defining an objective function, and introduces fuzzy dissimilarity to measure the differences and similarities between samples. FMC further considers the similarity between data points during the clustering process, more accurately characterising the complex structure of the data.

Assuming that the remote sensing image dataset $X = \{x_1, x_2, ..., x_n\}$ consists of k categories, with the centre of each cluster being $m_j\ (j = 1, 2, ..., k)$, the clustering loss function based on membership is represented by the following formula:

$$J_f = \sum_{j=1}^{k}\sum_{i=1}^{n}\left[\mu_j(x_i)\right]^b \left\| x_i - m_j \right\| \tag{20}$$

In formula (20), $\mu_j(x_i)$ represents the membership function of category j corresponding to the ith sample. The iterative formulas for m_j and $\mu_j(x_i)$ are as follows:

$$m_j = \frac{\sum_{i=1}^{n}\left[\mu_j(x_i)\right]^b x_i}{\sum_{i=1}^{n}\left[\mu_j(x_i)\right]^b} \tag{21}$$

$$\mu_j(x_i) = \frac{\| x_i - m_j \|^{-2/(b-1)}}{\sum_{s=1}^{k} \| x_i - m_s \|^{-2/(b-1)}} \tag{22}$$

After initialising the cluster centre, the membership function is calculated using formula (20), and the current membership function is used to recalculate the cluster center. When the algorithm converges, the final clustering result can be obtained.

3 *FDA module*

Using discrete cosine transform (DCT) as a frequency domain analysis tool (Gul and Toprak, 2023; Abbasi et al., 2022), remote sensing images can be divided into parts with different visual qualities. The formula for the variation of DCT is as follows:

$$f_m = \sum_{k=0}^{n-1} x_k cos\left[\frac{\pi}{n} m\left(k+\frac{1}{2}\right)\right] \tag{23}$$

In the above formula, x_k represents the kth remote sensing image, and m represents the clustering center. The one-dimensional DCT shown in formula (23) cannot meet the task requirements, so a two-dimensional DCT is introduced to handle the task. The forward transformation formula is given by the following formula:

$$f(u,v) = \sum\sum f(x,y) * \frac{\cos\left((2x+1)u\pi\right)}{2N} * \frac{\cos\left((2y+1)v\pi\right)}{2N} \tag{24}$$

In the above formula, $f(x,y)$ is a two-dimensional vector in the spatial domain, (u,v) represents the elements of the transformation coefficient array, (x,y) represents the spatial greyscale values of the original image, (u,v) is the frequency coordinates in the frequency domain.

This paper uses gated linear units to select the key components, and the output results are then obtained through two fully connected layers to obtain the difference diagram of remote sensing changes at different time points, thus achieving change detection of remote sensing images. The results are as follows:

$$h(X) = (X \times W + b) \odot \sigma(X \times V + c) \tag{25}$$

In the above formula, W and V represent different weight matrices, is σ represents the sigmoid function, b and c represent the calculation deviation of different elements, and $\odot$ represents the multiplication of each element.

2.4 Intelligent monitoring method for agricultural non-point source pollution

Based on the remote sensing image change detection results, combined with agricultural non-point source pollution monitoring indicators, intelligent technology can be used to achieve intelligent monitoring. This can improve monitoring efficiency, accuracy, and timeliness, and provide important information support for environmental protection departments and decision-makers.

The normalised vegetation index (NVI) is widely utilised as a crucial indicator in the monitoring and assessment of agricultural non-point source pollution. It offers valuable insights into the vegetation cover and growth status in agricultural areas.

$$N_{DVI} = (NIR - Red) / (NIR + Red) \tag{26}$$

In formula (26), *NIR* is the near-infrared reflectance, *Red* is the red reflectance.

The difference vegetation index (DVI) is extensively employed as a key indicator for monitoring agricultural non-point source pollution. It provides valuable information regarding vegetation growth and health status in agricultural areas. The specific calculation formula for DVI is as follows:

$$D_{VI} = NIR - Red \tag{27}$$

The green vegetation index specific calculation formula is as follows:

$$G_{VI} = Green / \left(Green + Red + Blue \right) \tag{28}$$

In the above formula, $Green$ is the reflectance in the green light band, $Blue$ is the reflectance in the blue light band.

Soil erosion indicators are essential tools in the monitoring. They are specifically designed to assess and monitor the severity of soil erosion in farmland. Soil erosion refers to the impact of external factors such as rainfall, water flow, and wind on the soil surface, resulting in the loss of soil particles and a decrease in soil quality. The indicator is calculated using the following formula.

$$E_I = \left(R * K * LS * C \right) / P \tag{29}$$

In the above formula, R is the rainfall erosivity factor, K is the land management factor, LS is the slope length factor, C is the coverage factor, and P is the protection measure factor.

The specific calculation formula for sediment transport rate in the soil loss model is as follows:

$$S_{SY} = \left(R * K * LS * C \right) / P \tag{30}$$

Chlorophyll concentration in water is an important parameter in water pollution indicators, used to evaluate and monitor algae growth and water quality in water bodies. The calculation formula for chlorophyll concentration in water based on regression models of measured and remote sensing data is as follows:

$$C_{hl-a} = a * Rrs + b \tag{31}$$

In the above formula, Rrs represents the far-infrared radiation reflectance, and a and b represent different regression coefficients.

The formula for calculating the concentration of suspended solids in water bodies is as follows:

$$T_{SM} = a * \left(Rrs - b \right)^c \tag{32}$$

In the above formula, c represents an empirical parameter that can be fitted through measured data.

To calculate dissolved oxygen, a spatial interpolation model based on remote sensing images is utilised. The specific calculation formula is as stated below:

$$D_O = k_1 * T + k_2 * C_{hl-a} + k_3 * S_h + k_4 * PAR \tag{33}$$

In the above formula, T represents water temperature, S_h represents transparency, P_A represents photosynthetic effective radiation, and k_1, k_2, k_3, and k_4 represent different weight coefficients.

The Moran's I index is employed in this paper to assess the level of spatial autocorrelation, which indicates the clustering of pollution. The precise calculation formula is provided below:

$$M_I = (n/W) * (X - X_{bar})' * W * (X - X_{bar}) / (X - X_{bar})' * (X - X_{bar}) \tag{34}$$

In formula (34), n is the number of remote sensing image samples, X is the variable values of remote sensing images, X_{bar} is the average value of the variables.

Through the amalgamation of agricultural non-point source pollution monitoring indicators mentioned earlier with the outcomes obtained from remote sensing image change detection, a sophisticated model for intelligent monitoring has been developed. The precise formulation of the intelligent monitoring model is as follows:

$$E = \sum_{i=1}^{n} \frac{r_i' + y_i y_j}{h(X)} \tag{35}$$

In the above formula, r_i' is abnormal parameters, y_i represents agricultural non-point source pollution load, and y_j is pollution concentration.

3 Experimental design

3.1 Experimental scheme

To validate the practicality of the intelligent monitoring method for agricultural non-point source pollution, a series of experimental tests were carried out.

Step 1: Determine the research area, develop an experimental plan based on the experimental subjects and research requirements, determine monitoring points, monitoring frequency, monitoring period, and sampling method. Figure 3 showcases the remote sensing images captured within the designated study area.

Figure 3 Remote sensing images of the study area (see online version for colours)

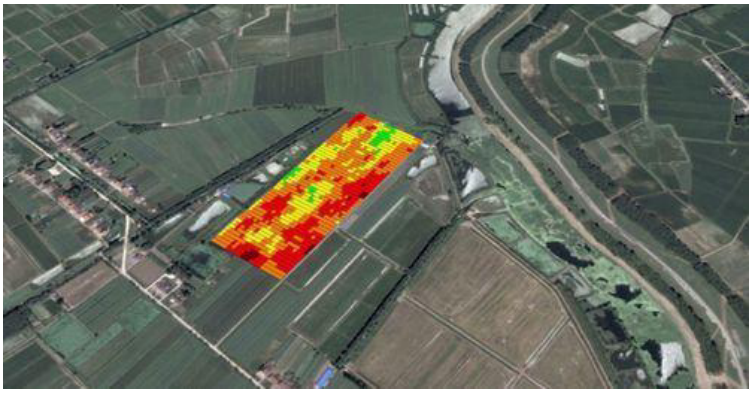

1 *Monitoring points*: Considerable attention was directed towards areas exhibiting potential or verified instances of agricultural non-point source pollution, notably encompassing farmland and the surrounding regions of aquaculture farms. Representative points were carefully chosen considering the feasibility and practicality of sampling operations.

2 *Monitoring frequency*: Determine the monitoring frequency based on the monitoring purpose and research requirements, and choose continuous and intermittent monitoring methods to achieve agricultural non-point source pollution monitoring.

3 *Monitoring period*: The monitoring period needs to be determined based on factors such as agricultural activities, seasonal changes, and hydrological and meteorological conditions.

4 *Sampling method*: Suitable sampling methods can be selected based on different monitoring objects, such as soil sample collection, water sample collection, crop leaf or root collection, etc.

Step 2: Install corresponding intelligent monitoring equipment or sensors, such as automatic weather stations, soil moisture monitors, water level and flow monitors, to ensure accurate data acquisition.

Step 3: Regularly collect data obtained from monitoring equipment, including parameters such as soil, hydrology, meteorology, plants, and water quality. Record the time, location, and relevant information of monitoring data, and the types of data collected are as follows:

1 Hydrological data: Including hydrological monitoring data such as water level, flow, rainfall, etc., used to understand changes in water bodies and water cycle conditions.

2 Soil data: In addition to the aforementioned factors, soil monitoring data including soil moisture, soil moisture content, and soil temperature were also incorporated to assess the soil moisture status and temperature variations.

3 *Meteorological data*: Moreover, for a comprehensive analysis, meteorological monitoring data, and wind direction were included to assess the impact of weather conditions on agricultural non-point source pollution.

4 *Plant data*: Includes plant monitoring data such as crop growth, crop leaf area index (LAI), and crop leaf nitrogen content, used to analyse plant growth status and nutrient utilisation.

5 *Water quality data*: Includes monitoring data on the concentration of pollutants such as nitrogen, phosphorus, and chemical oxygen demand (COD) in water bodies, used to evaluate the quality and degree of pollution of water bodies.

6 *GPS data*: Including the longitude and latitude coordinates of monitoring points, used to record the spatial position information of monitoring points.

Step 4: Clean, organise, and analyse the collected data accordingly.

Step 5: Input the obtained data into the simulation software, use different methods to complete the intelligent monitoring experiment of agricultural non-point source pollution, and obtain relevant experimental results.

The actual application effects of different methods are verified by comparing their monitoring coverage, pollutant concentration monitoring accuracy, and pollutant load monitoring accuracy. The coverage rate of the coverage of monitoring activities in a specific geographical area or agricultural activity range, and the higher the coverage rate, the more accurate the monitoring results obtained. The accuracy index for monitoring the concentration of agricultural non-point source pollutants is used to evaluate the consistency between monitoring results and actual pollutant concentrations. The accuracy index of agricultural non-point source pollutant load monitoring is used to evaluate the consistency between monitoring results and actual pollutant load values. The higher the accuracy of pollutant concentration monitoring and pollutant load monitoring, the more accurate the monitoring results are.

3.2 Experimental result

Figure 4 illustrates the comparison results of agricultural non-point source pollution monitoring coverage rates between the three experimental comparison methods.

Figure 4 Monitoring coverage rate (see online version for colours)

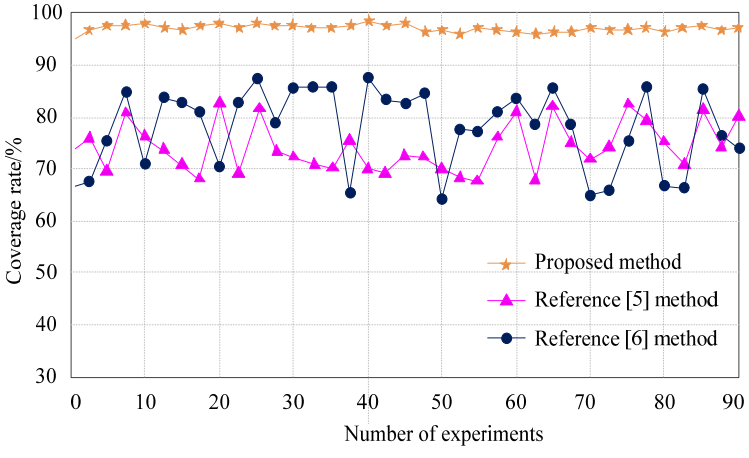

As the number of experiments increases, the monitoring coverage rate by the three methods shows a fluctuating trend. Among them, compared with the three experimental methods has a more stable monitoring coverage curve fluctuation, indicating that the monitoring process of this method is more stable. From a data perspective, the monitoring coverage rate using Zhang et al. (2022) method is 67.2% to 83.12%; the monitoring coverage rate using Wang and Li (2022) method is 64.9~86.2%; the monitoring coverage rate using the proposed method is above 96.3%, indicating that the monitoring coverage rate for this method is higher, indicating that this method can more accurately understand and grasp the potential impact of agricultural activities on the environment, and timely detect and solve potential non-point source pollution problems.

Table 2 presents the comparison results of the accuracy of pollutant concentration monitoring between the three experimental comparison methods.

Table 2 Accuracy of monitoring the concentration of agricultural non-point source pollutants

Number of experiments	*Accuracy of pollutant concentration monitoring/%*		
	Reference Zhang et al. (2022) method	*Reference Wang and Li (2022) method*	*Proposed method*
10	86.2	65.8	96.7
20	82.5	67.4	95.8
30	74.9	74.1	97.4
40	82.3	75.2	98.3
50	78.5	74.3	97.1
60	80.3	76.5	96.3
70	82.6	77.1	97.5
80	84.1	69.8	98.5
90	83.2	66.3	96.4
Mean value	81.6	71.8	97.1

The maximum accuracy of monitoring the concentration of agricultural non-point source pollutants using Zhang et al. (2022) method is 86.2%, the maximum accuracy of monitoring the concentration of pollutants using Wang and Li (2022) method is 77.1%, and the maximum accuracy of monitoring the concentration of pollutants using the proposed method is 98.5%; The minimum accuracy of monitoring the concentration of agricultural non-point source pollutants in Zhang et al. (2022) method is 74.9%, the minimum accuracy of monitoring the concentration of pollutants in Wang and Li (2022) method is 65.8%, and the minimum accuracy of monitoring the concentration of pollutants in the proposed method is 95.8%; The average accuracy of monitoring the concentration of agricultural non-point source pollutants using Zhang et al. (2022) method is 81.6%, the average accuracy of monitoring the concentration of pollutants using Wang and Li (2022) method is 71.8%, and the average accuracy of monitoring the concentration of pollutants using the proposed method is 97.1%. Overall, the proposed method has the highest accuracy in monitoring the concentration of agricultural non-point source pollutants, indicating that it can more accurately measure and analyse the concentration of non-point source pollutants in agricultural production processes. This helps to more accurately understand the potential impact of agricultural activities on the environment and can formulate more scientific and refined environmental protection and agricultural management policies.

Table 3 exhibits the comparison results of the accuracy of agricultural non-point source pollutant load monitoring between the three experimental methods.

The maximum accuracy of agricultural non-point source pollutant load monitoring using Zhang et al. (2022) method is 88.3%, the average is 83.6%, and the minimum value is 80.6%. The maximum accuracy of agricultural non-point source pollutant load monitoring using Wang and Li (2022) method is 78.9%, the average is 74.4%, and the minimum value is 70.1%. The maximum accuracy of the proposed method for monitoring agricultural non-point source pollutant load is 99.3%, the average is 97.6%, and the minimum value is 94.7%. From various angles, the proposed method demonstrates the highest accuracy in monitoring agricultural non-point source pollutant load. This indicates that it has the potential to achieve precise and reliable monitoring.

Table 3 Accuracy rate of agricultural non-point source pollutant load monitoring

Number of experiments	*Accuracy of pollutant load monitoring/%*		
	Zhang et al. (2022) method	*Wang and Li (2022) method*	*Proposed method*
10	82.3	75.6	98.5
20	80.6	74.1	97.4
30	85.2	75.2	98.2
40	84.1	77.3	98.5
50	86.3	74.6	99.3
60	82.7	78.9	94.7
70	80.6	74.6	97.2
80	81.9	72.3	96.3
90	88.3	70.1	98.1
Mean value	83.6	74.4	97.6

4 Conclusion

Indeed, agricultural non-point source pollution poses significant damage and threats to the water environment and ecosystem. By monitoring pollution, we can effectively detect and control the sources of pollution in the early stages, allowing for prompt intervention and mitigation measures to protect and preserve the water environment and ensure the sustainability of the ecosystem. Aiming at the problems of traditional monitoring methods, an intelligent monitoring method for agricultural non-point source pollution based on remote sensing image changes is proposed. The test findings demonstrate that the proposed method achieves a remarkable coverage rate of over 96.3% when monitoring agricultural non-point source pollution, an average accuracy rate of 97.1% for pollutant concentration monitoring, and a maximum accuracy rate of 99.3% for pollutant load monitoring. This indicates that the method can achieve precise monitoring. Through continuous research work, the proposed method in this paper will continue to play an important role and make greater contributions to sustainable agricultural development and environmental protection.

Acknowledgements

This work was supported by Jiangsu Province Industry-University-Research Co-operation Project no. BY2022972,and Major Project of Basic Science (Natural Science) Research in Jiangsu Higher Education Institutions no. 23KJA520005, and Jiangsu Food & Pharmaceutical Science College Mei Cheng scholar Program.

References

Abbasi, B.S., Vali, M. and Modaresi, M. (2022) 'Noise reduction of lung sounds based on singular spectrum analysis combined with discrete cosine transform', *Applied Acoustics*, Vol. 199, No. 10, pp.157–173.

Fan, L., Yang, J., Sun, X., Niu, Z. and Li, Y.L.(2022) 'The effects of Landsat image acquisition date on winter wheat classification in the North China plain', *ISPRS Journal of Photogrammetry and Remote Sensing*, Vol. 187, May, pp.1–13.

Gul, E. and Toprak, A.N. (2023) 'Contourlet and discrete cosine transform based quality guaranteed robust image watermarking method using artificial bee colony algorithm', *Expert Systems with Application*, Vol. 213, No. 2, pp.1–16.

Li, H., Wu, G., Xu, F., Guo, J. and Ren, B.C. (2011) 'Landsat-8 and gaofen-1 image-based inversion method for the downscaled land surface temperature of rare earth mining areas', *Infrared Physics and Technology*, Vol. 113, No. 10, pp.103658–103668.

Li, X.P., Cai, J., Wang, Q.J., Ning, M.B. and He, F.(2022) 'Heterogeneous public preferences for controlling agricultural non-point source pollution based on a choice experiment', *Journal of Environmental Management*, Vol. 305, No. 1, pp.114413–114420.

Lin, J. and Pan, J. (2020) 'Farmers' Willingness as well as its compensation strategy to prevent and control agricultural non-point source pollution in water source areas-based on a comparative analysis of pesticide and fertilizer inputs, *International Journal of Sustainable Development and Planning: Encouraging the Unified Approach to Achieve Sustainability*, Vol. 15, No. 8, pp.1303–1311.

Niu, Z., Yi, F. and Chen, C. (2022) 'Agricultural insurance and agricultural fertilizer non-point source pollution: evidence from China's policy-based agricultural insurance pilot', *Sustainability*, Vol. 14, No. 5, pp.1–10.

Ridwana, R., Sugandi, D., Arrasyid, R. (2021) 'Multitemporal Landsat image utilization for spatial prediction of built up area in Tasikmalaya city, Indonesia', *IOP Conference Series: Earth and Environmental Science*, Vol. 683, No. 1, pp.012101–012110.

Shirazi, D.H. and Toosi, H. (2023) 'Deep multilayer perceptron neural network for the prediction of Iranian dam project delay risks', *Journal of Construction Engineering and Management 2023*, Vol. 149, No. 4, pp.1–13.

Wan, F. (2021) 'Application of the source-sink landscape method in the evaluation of agricultural non-point source pollution: first estimation of an orchard-dominated area in China', *Agricultural Water Management*, Vol. 252, No. 1, pp.1–10.

Wang, X.Y. and Li, H. (2022) 'A water pollution monitoring method based on graph convolutional neural network', *Electronic Technology and Software Engineering*, Vol. 23, No. 7, pp.212–215.

Wu, Y., Jia, Y., Ning, X., Wan, F. and Du, H.K.(2022) 'Detection of pediatric obstructive sleep apnea using a multilayer perceptron model based on single-channel oxygen saturation or clinical features', *Methods (San Diego, Calif.)*, Vol. 204, No. 1, pp.361–367.

Xiang, L.J., Zheng, Y.M. and Hong, X.M. (2022) 'Development of distributed online monitoring and early warning system for water pollution based on cloud platform of internet of things', *Industrial Control Computer*, Vol. 35, No. 12, pp.70–73.

Zhang, L.J., Lv, D.Z., Gao, Y.Q., He, Y. and Luo, K. (2022) 'Design and simulation of remote sensing monitoring method for water pollution', *Computer Simulation*, Vol. 39, No. 6, pp.289–292, 312.

Zhao, X., Wu, J., Wang, H., Chen, K.L. and Feng, J. (2022) 'Injecting spectral indices to transferable convolutional neural network under imbalanced and noisy labels for Landsat image classification', *International Journal of Digital Earth*, Vol. 15, No. 1, pp.26–39.